18th International Conference on Information Fusion
Washington, DC - July 6-9, 2015

Improved Multi-Focus Image Fusion

Amina Jameel
Department of Computer Engineering
Bahria University
Islamabad
Email: aminajameel.bahria@gmail.com

Fouzia Noor
Department of Electrical Engineering
Bahria University
Islamabad
Email: fouzianoor2010@hotmail.com

***Abstract*—A two scale image fusion scheme for multi focus images is proposed. The source images are decomposed into base and detail layers. The base layers contain the large scale variations and are averaged out to obtain the base layer of the fused image. The weights of detail layers are computed based on whether the object in a particular image is in focus compared to the same object in the other image. Simulation results reveal the significance of proposed scheme.**

I. Introduction

Well focused images are more useful in image processing, remote sensing, and robotics applications than those with fewer focused objects [1]. The amount/quality of information in the captured images is directly affected by the contained depth of optical systems. The objects in the illustrated scene will be defocused if they fall outside the effective depth of field (EDOF) limits [2]. Since effective depth of field (EDOF) limits the objects in focus of the illustrated scene proportionally [2]. So the EDOF of optical systems need to be enhanced by taking multiple images of the same illustrated scene but with different focus settings and fusing them finally to get one composite image which is better in focus and quality [3].

Previously a lot of work has been done to improve the EDOF of optical systems. Multiresolution (pyramid or wavelet transform) fusion techniques [4]-[5] are based on the fact that image contains relevant features at different scales. Gradient pyramid and variance (for activity measure) produces blocking effects in the fused image [4]. Discrete wavelet transform (DWT) based multisource image fusion using spatial frequency and simplified pulse coupled neural network suffers from shift variance (because of downsamplers) [6]-[8]. Multiscale geometric analysis tools (curvelet transform [9], contourlet transform (CT) [10]) obtain the asymptotic optimal representation by taking advantage of the geometric regularity of image intrinsic structures. Localization, multidirection, and anisotropy are the characteristics of CT [11]. However, it does not possess the shift-invariance property resulting in artifacts along the edges to some extent [11].

Non subsampled contourlet transform (NSCT) selects the lowpass and highpass coefficients (using sum-modified laplacian and local neighbour sum of laplacian) to obtain the fused image [8]. Similarly a NSCT based multi-focus fusion combines the advantages of transformed and spatial domain methods [11]. Surfacelet transform and compound pulse-coupled neural network selects the fusion coefficients in an optimized fashion [12]. Multi-scale weighted gradient-based fusion technique minimizes the problem of anisotropic blur and mis-registration [13]. The limitations of these schemes include computationally complexity and less robustness [14].

Robust principal component analysis and local sparse features assumes sparse nature of images [15]. A block based image fusion uses a quad-tree structure to obtain an optimal subdivision of blocks [16]. *Pertuz et al.* [2] proposed a selective all-in-focus algorithm (SAF) for fusion of noisy images. The technique is based on three step procedure (measure, selectivity and fusion). The SAF [2] all in focus image obtained appears to be blurry in some portions of the image, hence some of the details are enhanced while others are flattened out. Recently, Guided Filter Fusion (GFF) [17] is used to preserve edges and avoiding blurring effects in the fused image. Guided filter is an edge-preserving filter and its computational time is also independent of filter size. However, the method provides limited performance due to the use of gaussian filter and two level weight maps.

To overcome the above issues, a two scale image fusion scheme is proposed for multi-focus images. Source images are decomposed into base and detail layers. The base layers of the source images are averaged out to obtain the base layer of the fused image. The detail layers weights are computed based on whether the object in a particular image is in focus compared to the same object in all other images. Simulation results clearly indicate that our proposed scheme is more efficient, accurate and provide halo free results comparable to state of the art schemes. The salient features of the proposed scheme include: it is based on a two scale decomposition method; algorithm is simple and robust, computationally efficient and an improved image quality.

II. Proposed Image Fusion

Let I_F be the fused image obtained by combining input images, I_k where $k = 1, 2$ having dimensions $M \times N$ of the same scene with different focus settings. The source images are decomposed into base I_B and detail I_D layers [18].

$$\begin{aligned} I_{B_k} &= I_k \times f \\ I_{D_k} &= I_k - B_k \end{aligned} \tag{1}$$

where I_k represents the two source images, I_{B_k} and I_{B_k} are the base and detail layers of the k^{th} source image respectively,

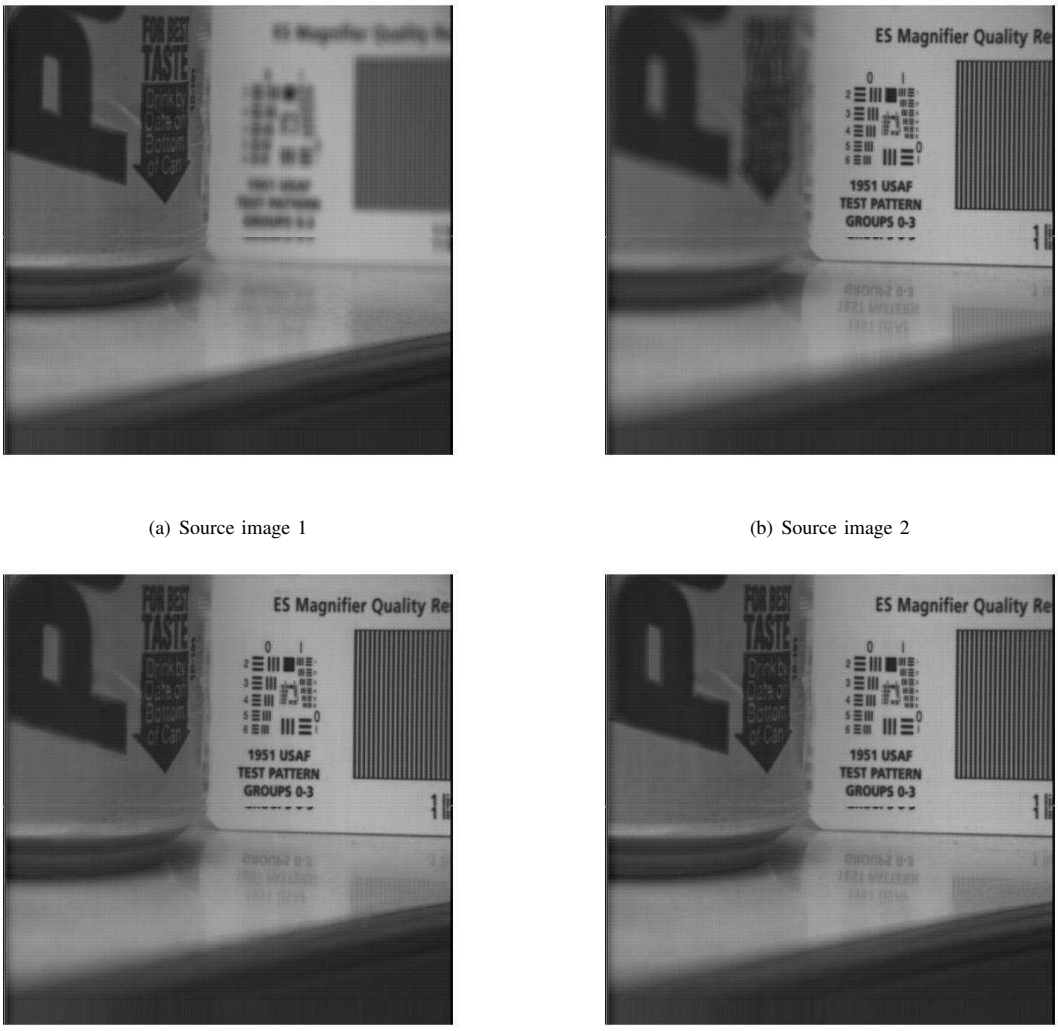

(a) Source image 1

(b) Source image 2

(c) GFF [21] fused image

(d) Proposed fused image

Fig. 1. Example 1: Visual comparison of proposed and GFF [21] fusion schemes

and f is the average filter of size 31×31. The base and detail layers contain large and small scale variations respectively.

A. Base Layer Weight Map Assignment

The decomposition process is then followed by the appropriate assignment of weights to these layers. The base layers of all the images contain the large scale variations and are averaged out to obtain the base layer of the fused image.

$$I_{B_F} = \frac{1}{2}\sum_{k=1}^{2} I_{B_k} \tag{2}$$

where I_{B_F} represents the base layer of the fused image. The averaging process also helps to smooth the noise.

B. Detail Layer Weight Map Assignment

The detail layer weight maps are computed based on whether an object in an image is in focus as compared to the same object in the other image. A wavelet based focus measure is used to calculate these weights. The focus measure (based on sum of wavelet coefficients) reflects the statistical properties of images. The wavelet coefficients W^{LL}, W^{LH}, W^{HL}, and W^{HH} are,

$$I_1 \xrightarrow[1^{st}\text{ Level}]{\text{Wavelet Transform}} \left(W_1^{LL}, W_1^{LH}, W_1^{HL}, W_1^{HH}\right) \tag{3}$$

$$I_2 \xrightarrow[1^{st}\text{ Level}]{\text{Wavelet Transform}} \left(W_2^{LL}, W_2^{LH}, W_2^{HL}, W_2^{HH}\right) \tag{4}$$

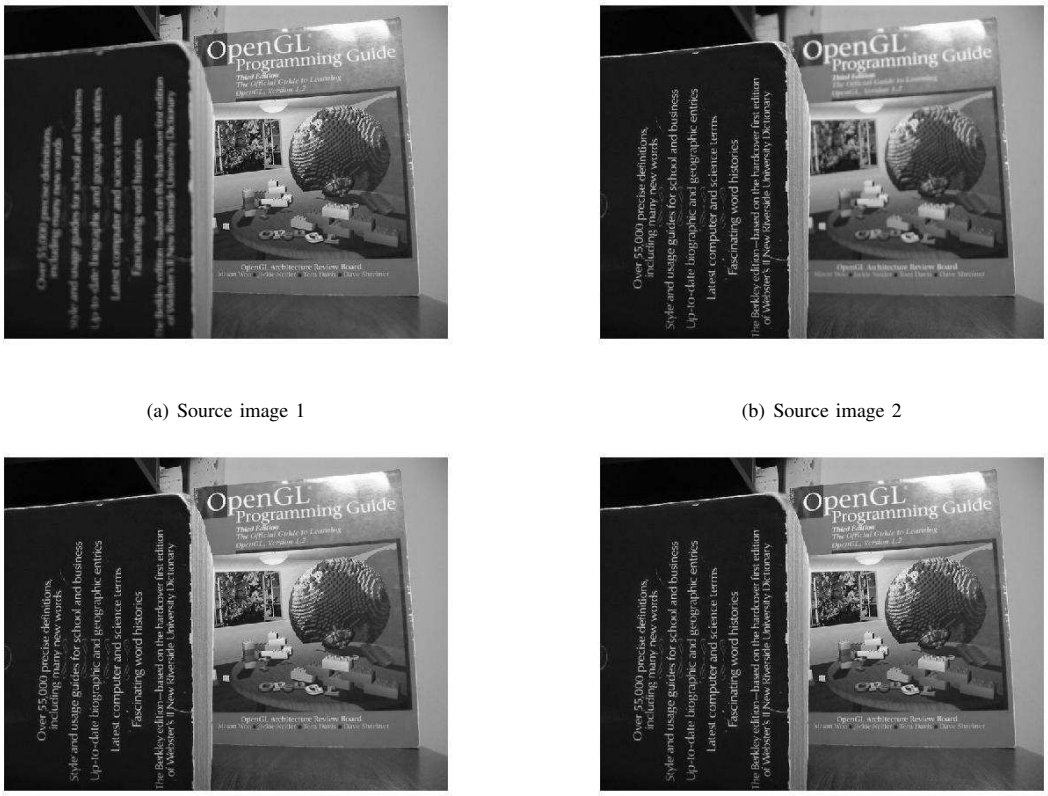

(a) Source image 1

(b) Source image 2

(c) GFF [21] fused image

(d) Proposed fused image

Fig. 2. Example 2: Visual comparison of proposed and GFF [21] fusion schemes

The focus measures ψ_1 and ψ_2, based on sum of wavelet coefficients are [2], [19],

$$\psi_1(m,n)=\frac{\sum_{i_1,i_2}\left(\bar{W}_1^{LH}(i_1,i_2)+\bar{W}_1^{HL}(i_1,i_2)+\bar{W}_1^{HH}(i_1,i_2)\right)}{3(m_1\times n_1)} \quad (5)$$

$$\psi_2(m,n)=\frac{\sum_{i_1,i_2}\left(\bar{W}_2^{LH}(i_1,i_2)+\bar{W}_2^{HL}(i_1,i_2)+\bar{W}_2^{HH}(i_1,i_2)\right)}{3(m_1\times n_1)} \quad (6)$$

where $m-\left\lfloor\frac{m_1}{2}\right\rfloor \le i_1 \le m+\left\lfloor\frac{m_1}{2}\right\rfloor$ and $n-\left\lfloor\frac{n_1}{2}\right\rfloor \le i_2 \le n+\left\lfloor\frac{n_1}{2}\right\rfloor$ and $m_1\times n_1$ is the window size. $\left\{\bar{W}_1^{LH},\bar{W}_1^{HL},\bar{W}_1^{HH}\right\}$ and $\left\{\bar{W}_2^{LH},\bar{W}_2^{HL},\bar{W}_2^{HH}\right\}$ are the mean value of wavelet coefficients. These focus measure reflects the statistical properties (like energy and strength) of the wavelet coefficients in high frequency subbands.

The focus maps are then scaled and converted into binary images $\acute{\psi}_1$ and $\acute{\psi}_2$ i.e.,

$$\acute{\psi}_1(m,n)=\begin{cases}1 & \text{if} \quad \psi_1(m,n)\ge\psi_2\\ 0 & otherwise\end{cases} \quad (7)$$

Similarly,

$$\acute{\psi}_2(m,n)=\begin{cases}1 & \text{if} \quad \psi_2(m,n)\ge\psi_1\\ 0 & otherwise\end{cases} \quad (8)$$

The morphological closing is then performed on binary images with a structuring element B to generate the detail layer weight maps.

$$\Gamma_1^D=\acute{\psi}_A(m,n)\bullet B \quad (9)$$

$$\Gamma_2^D=1-\Gamma_1^D \quad (10)$$

C. Fusion

The fused detail layer I_{D_F} is obtained as [18],

$$I_{D_F}=\sum_{k=1}^{2}\Gamma_k^D\times I_{D_k} \quad (11)$$

The fused base and detail layers are combined to obtain the fused image. The fused image I_F is,

$$I_F=I_{B_F}+I_{D_F} \quad (12)$$

The proposed algorithm is robust against noise (since averaging is done on the base layers) and enhances the details

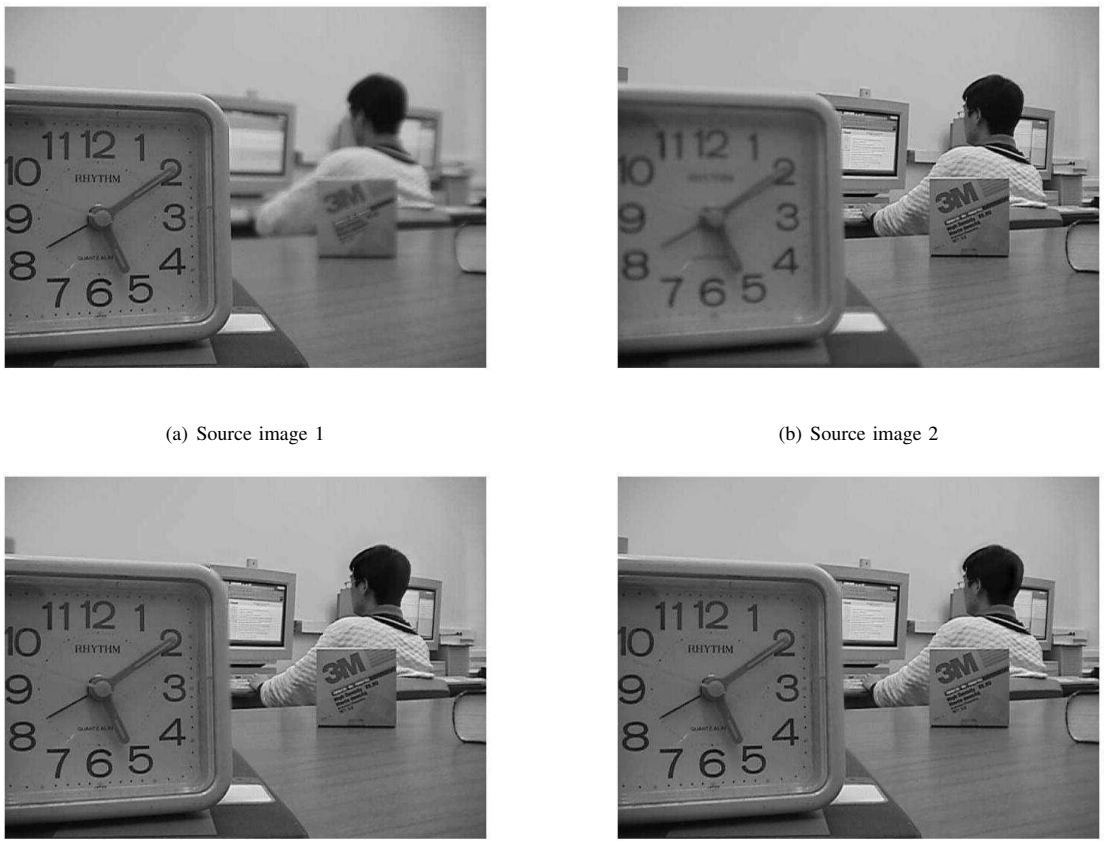

(a) Source image 1

(b) Source image 2

(c) GFF [21] fused image

(d) Proposed fused image

Fig. 3. Example 3: Visual comparison of proposed and GFF [21] fusion schemes

(by giving specific weights to each detail layer) and produces halo free results.

III. Results and Analysis

The proposed technique is verified on several pairs of multi-focus source images [20] and it is compared with GFF [21] scheme. For quantitative evaluation, different measures including mutual information measure ζ_{MI}, structural similarity measure ζ_{SSIM}, Piella and Heijmans measures ζ_{P_1} and ζ_{P_2} and visual information fidelity fusion metric ζ_{VIFF} are considered [22]. The quality metric ζ_{MI} evaluates the amount of information transfer from source images into the fused image. ζ_{SSIM} is a measure indicating the structural information transfer into the fused image. ζ_{P_1} and ζ_{P_2} estimate the presence of the salient information in the fused image. A higher value of these measures indicate a better fusion result.

A. MI Measure

MI is a statistical measure which provides the degree of dependencies in different images. Large value of MI implies better quality and vice versa [23].

$$\zeta_{\text{MI}} = \frac{2}{(H_{I_1} + H_{I_F})} \sum_{I_1, I_F} P_{1\text{F}}(I_1, I_F) \log \frac{P_{1\text{F}}(I_1, I_F)}{P_1(I_1) P_{\text{F}}(I_F)} + \frac{2}{(H_{I_2} + H_{I_F})} \sum_{I_2, I_F} P_{2\text{F}}(I_2, I_F) \log \frac{P_{2\text{F}}(I_2, I_F)}{P_2(I_2) P_{\text{F}}(I_F)} \quad (13)$$

where H_{I_1}, H_{I_2}, and H_{I_F} are the entropy of I_1, I_2, and I_F images respectively. $P_{1\text{F}}$ is the jointly normalized histogram of I_1 and I_F, $P_{2\text{F}}$ is the jointly normalized histogram of I_2 and I_F, P_1, P_2 and P_{F} are the normalized histogram of I_1, I_2 and I_F respectively.

B. SSIM [24] Measure

SSIM [24] measure evaluates the amount of structural information transfer into the fused image. Higher SSIM values indicate a higher quality fused image. It is defined as,

$$\zeta_{\text{SSIM}}(I_1, I_2, I_F) = \begin{cases} \lambda_w \zeta_{\text{SSIM}}(I_{1_w}, I_{F_w}) + (1 - \lambda_w) \zeta_{\text{SSIM}}(I_{2_w}, I_{F_w}) \\ if \;\; \zeta_{\text{SSIM}}(I_{1_w}, I_{2_w} | w) \geq 0.75 \end{cases} \quad (14)$$

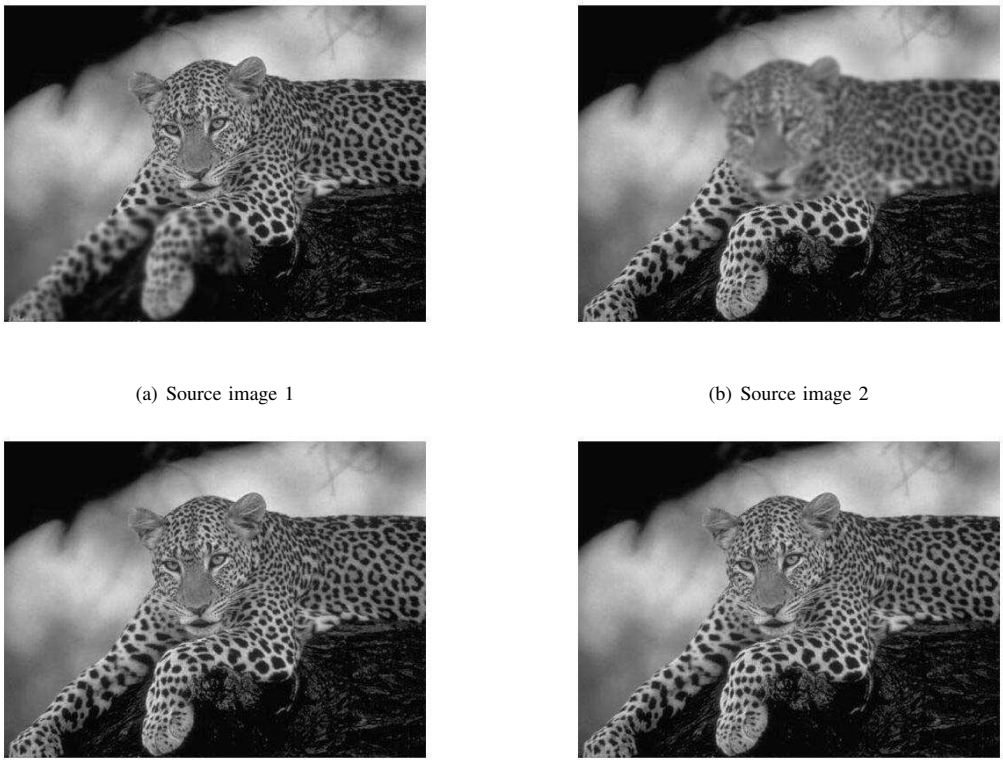

(a) Source image 1

(b) Source image 2

(c) GFF [21] fused image

(d) Proposed fused image

Fig. 4. Example 4: Visual comparison of proposed and GFF [21] fusion schemes

TABLE I
QUANTITATIVE ANALYSIS OF GFF [21] AND PROPOSED SCHEMES

Quantitative Measures	Example 1		Example 2		Example 3		Example 4	
	GFF [21]	Proposed	GFF [21]	Proposed	GFF [21]	Proposed	GFF [21]	Proposed
ζ_{MI}	1.013	1.039	1.0879	1.1888	1.0683	1.1642	1.3826	1.4516
ζ_{SSIM}	0.9553	0.9581	0.9509	0.9619	0.9519	0.9615	0.9920	0.9931
ζ_{P_1}	0.9595	0.9685	0.9436	0.9487	0.9503	0.9561	0.9738	0.9742
ζ_{P_2}	0.9590	0.9608	0.9180	0.9215	0.9276	0.9331	0.9586	0.9591
ζ_{VIFF}	0.8806	0.9006	0.8549	0.8585	0.9049	0.9147	0.9956	0.9968

$$\zeta_{\text{SSIM}}(I_1, I_2, I_F) = \begin{cases} \max(\zeta_{\text{SSIM}}(I_{1_w}, I_{F_w}), \zeta_{\text{SSIM}}(I_{2_w}, I_{F_w})) \\ if\ \ \zeta_{\text{SSIM}}(I_{1_w}, I_{2_w}|w) < 0.75 \end{cases} \tag{15}$$

where w is a sliding window and $\lambda(w)$ is,

$$\lambda_w = \frac{\sigma_{1_w}}{\sigma_{1_w} + \sigma_{2_w}} \tag{16}$$

σ_{1_w} and σ_{2_w} are the variance of images I_1 and I_2 respectively.

C. Piella and Heijmans [22] metric

Piella and Heijmans [22] metrics ζ_{P_1} and ζ_{P_2} are defined as,

$$\zeta_{P_1} = \frac{1}{|W|} \sum_{w \in W} [\lambda(w) Q_o(I_1, I_F|w) + (1 - \lambda(w)) Q_o(I_2, I_F|w) \tag{17}$$

$$\zeta_{P_2} = \sum_{w \in W} c(w)[\lambda(w) Q_o(I_1, I_F|w) + (1 - \lambda(w)) Q_o(I_2, I_F|w) \tag{18}$$

$Q_o(I_1, I_F|w)$ and $Q_o(I_2, I_F|w)$ are the local quality indexes calculated in a sliding window w, $\lambda(w)$ is defined as in eq. (13).

$$Q_o(A, F|w) = \frac{4\sigma_{1F}\bar{I_1}\bar{I_F}}{(\bar{I_1}^2 + \bar{I_F}^2 + (\sigma_{I_1}^2 + \sigma_{I_F}^2)} \tag{19}$$

where $\bar{I_1}$ is the mean of I_1, $\sigma_{I_1}^2$ and σ_{1F} are the variance of I_1 and the covariance of I_1, I_2 respectively.

$$c_w = \frac{\max[\sigma_{1_w}, \sigma_{2_w}]}{\sum_{w' \in W}[\sigma_{1'_w}, \sigma_{2'_w}]} \tag{20}$$

σ_{1_w} and σ_{2_w} are the variance of images I_1 and I_2 within the window w respectively.

D. VIFF [25] metric

VIFF [25] is a multi-resolution image fusion metric used to assess fusion performance objectively. It has four stages: (1) Source and fused images are filtered and divided into blocks. (2) Visual information is evaluated with and without distortion information in each block. (3) The VIFF of each sub-band is calculated and the overall quality measure is determined by weighting (of VIFF at different sub-bands).

Fig. 1 shows a pair of pepsi images with different spatial focuses. Fig. 1 (a) is a left focused image in which the can is in focus (clear). Fig. 1 (b) is a right focused image. The clear information from both the images should be transferred into the fused image. The fused image (Fig. 1(c)) obtained by GFF [21] scheme contain some halo effects. Clear halos can be seen around the text in the upper right corner of the image. However, there are no halos in the fused imaged obtained by the proposed scheme. The improvement in the quality of the fused image using the proposed scheme can be observed in Fig. 1(d).

Fig. 2 shows a pair of book images with different spatial focuses. Fig. 2 (a) is a right focused image in which the title page is in focus (clear). Fig. 2 (b) is a left focused image. The clear information from both the images should be transferred into the fused image. The fused image (Fig. 2 (c)) obtained by GFF [21] scheme and the proposed fused image (Fig. 2 (d)) appear almost similar. However, quantitative analysis show the superiority of the proposed scheme.

Fig. 3 shows another pair of blurred images. The fused image obtained using proposed scheme in Fig. 3 (d) again shows better results as compared to the fused images obtained by [21] scheme in Fig. 3 (c). Slight blurring can be seen in the upper left corner part of the image in Fig. 3 (c) which is not present in the proposed fused image (Fig. 3 (d)).

Fig. 4 shows a pair of tiger images with different spatial focuses. Fig. 4 (a) is a right focused image in which the right part of the lion is in focus (clear). Fig. 4 (b) is a left focused image. The clear information from both the images should be transferred into the fused image. The fused image (Fig. 4 (c)) obtained by GFF [21] scheme and the proposed fused image (Fig. 4 (d)) appear almost similar. However, quantitative analysis show the superiority of the proposed scheme.

TABLE I shows that proposed scheme provides better results in terms of ζ_{MI}, ζ_{SSIM}, ζ_{P_1}, ζ_{P_2} and ζ_{VIFF} as compared to existing GFF [21] scheme.

IV. Conclusion

A two scale image fusion scheme for multi focus images is proposed. The source images are decomposed into base and detail layers. The base layers contain the large scale variations and are averaged out to obtain the base layer of the fused image. The weights of detail layers are computed based on whether the objects in a particular image is in focus compared to the same object in all other images. Experimental results has shown that the proposed scheme can very well preserve the information from original source images without introducing halo and artifacts. Simulation results reveal the significance of the proposed scheme.

References

[1] S. Li, and B. Yang, 'Multifocus image fusion by combining curvelet and wavelet transform," *Pattern Recognition Letters*, vol. 29, no. 9, pp. 1295-1301, 2008.

[2] S. Pertuz, D. Puig, M. Garcia, and A. Fusiello, "Generation of all-in-focus images by noise-robust selective fusion of limited depth-of-field images," *IEEE Transactions on Image Processing*, vol. 22, no. 3, pp. 1242-1251, 2013.

[3] I. De, B. Chanda, and B. Chattopadhyay, "Enhancing effective depth-of-field by image fusion using mathematical morphology," *Image and Vision Computing*, vol. 24, no. 12, pp 1278-1287, 2006.

[4] P. J. Burt, and R. J. Kolezynski, "Enhanced image capture through fusion," *International Conference on Computer Vision*, Berlin, Germany, pp. 173-182, 1993.

[5] X. Yang, W. Yang, and J. Pei, "Different focus points images fusion based on wavelet decomposition," *International Conference on Information Fusion*, Paris, France, vol. 1, pp. 3-8, 2000.

[6] N. Wang, W. Wang, and X. Guo, "Multisource image fusion based on DWT and simplified pulse coupled neural network. Applied Mechanics and Materials, 457, 736-740, 2014.

[7] N. Wang, Y. Ma, and W. Wang, "DWT-based multisource image fusion using spatial frequency and simplified pulse coupled neural network,"*Journal of Multimedia*, vol. 9 ,no. 1, pp. 159-165, 2014.

[8] P. Geng, Z. Gao, and C. Hu, "Multi-focus Image Fusion using the local neighbor num of laplacian in NSCT domain," *International Journal of Signal Processing, Image Processing and Pattern Recognition*, vol. 6, no. 4, pp. 69-80, 2013.

[9] M. Choi, R. Kim, and M. Kim, "The curvelet transform for image fusion." *International Society for Photogrammetry and Remote Sensing*, vol. 35, pp. 59-64, 2004.

[10] M. N. Doa, and M. Vetterli," The contourlet transform: an efficient directional multiresolution image representation," *IEEE Transactions on Image Processing*, vol. 14, no. 12, pp. 2091-2106, 2005.

[11] H. Li, Y. Chai, and Z. Li, "Multi-focus image fusion based on non-subsampled contourlet transform and focused regions detection," *Optik-International Journal for Light and Electron Optics*, vol. 124, no. 1, pp. 40-51, 2013.

[12] B. Zhang, C. Zhang, L. Yuanyuan, W. Jianshuai, and L. He, "Multi-focus image fusion algorithm based on compound PCNN in surfacelet domain," *Optik-International Journal for Light and Electron Optics*, vol. 125, no. 1, pp. 296-300, 2014.

[13] Z. Zhou, S. Li, and B. Wang, "Multi-scale weighted gradient-based fusion for multi-focus images, Information Fusion, 2014, http://dx.doi.org/10.1016/j.inffus.2013.11.005.

[14] Y. Liu, J. Jin, Q. Wang, Y. Shen, and X. Dong,"Region level based multi-focus image fusion using quaternion wavelet and normalized cut," *Signal Processing*, vol. 97, pp. 9-30, 2014.

[15] T. Wan, C. Zhu, and Z. Qin,"Multifocus image fusion based on robust principal component analysis," *Pattern Recognition Letters*, vol. 34, no. 9, pp. 1001-1008, 2013.

[16] I. De, and B. Chanda,"Multi-focus image fusion using a morphology-based focus measure in a quad-tree structure," *Information Fusion*, vol. 14, no. 2, pp. 136-146, 2013.

[17] S. Li, X. Kang, and Jianwen Hu"Image Fusion with Guided Filtering", *IEEE Transactions on Image Processing*, Vol. 22, No. 7, July 2013.

[18] A. Jameel, and A. Ghafoor, and M. M. Riaz, "Improved guided image fusion for magnetic resonance and computed tomography imaging", *The Scientfic World Journal*, pp. 1-7, 2014.

[19] G. Yang, and J. Nelson, "Wavelet-based autofocusing and unsupervised segmentation of microscopic images", *IEEE/RSJ International Conference on Intelligent Robots and Systems*, vol. 3, 2003.

[20] Online databases at http://www.ucassdl.cn/resource.asp and http://dsp.etfbl.net/mif/

[21] S. Li, X. Kang, and J. Hu, "Image fusion with guided filtering," *IEEE Transactions on Image Processing*, vol. 22, no. 7, 2013.

[22] Z. Liu, E. Blasch, Z. Xue, J. Zhao, R. Laganiere, and W. Wu, 11Objective assessment of multiresolution image fusion algorithms for context enhancement in night vision: a comparative study," *IEEE Transactions on Pattern Analysis and Machine Intelligence*, vol. 34, pp. 94-109, 2012.
[23] M. Hossny, S. Nahavandi, and D. Creighton, "Comments on information measure for performance of image fusion," *Electronic Letters*, vol. 44, no. 18, pp. 1066-1067, 2008.
[24] C. Yang, J. Zhang, X. Wang, and X. Liu, "A novel similarity based quality metric for image fusion, *Information Fusion*, vol. 9, no. 2, pp. 156-160, 2008.
[25] Y. Han, Y. Cai, Y. Cao, and X. Xu, "A new image fusion performance metric based on visual information fidelity," *Information Fusion*, vol. 14, no. 2, pp. 127-135, 2013.